Research Article

Bashra Kadhim Oleiwi* and Mohamed Jasim Mohamed

Optimal design of linear and nonlinear PID controllers for speed control of an electric vehicle

https://doi.org/10.1515/jisys-2024-0028
received January 09, 2024; accepted June 16, 2024

Abstract: Electric vehicles (EVs) as a sustainable safety system are being increasingly used and receiving attention from researchers for several reasons including optimal performance, affordability for consumers, and environmental safety. EV speed control is a crucial issue that requires reliable and intelligent controllers for maintaining this matter. The primary goal of this research is to design the linear and nonlinear Proportional, Integral, and Derivative (PID) controllers to control EV speed based on the minimum value of ITAE plus ISU (integral square of control signal) as well as satisfy the constrain on response overshoot. All the proposed PID controllers, conventional PID controller, arc tan PID controller, and nonlinear PID controller (NL-PID) are used in cascade with EV model. In all these PID controllers, a filter is used with the derivative term to avoid the effect of the noise. The tuning of the proposed controller gains is achieved using Aquila Optimization algorithm. The controllers' parameter tuning is primarily determined by reducing the Integral Time Absolute Error (ITAE) and integral square control signal. Numerical simulation, system modelling, and controller design are done using MATLAB. By comparing the results, the proposed controllers' efficacy is demonstrated. The proposed NL-PID controller provides promising EV speed regulation control and robustness to external disturbances. Where, the performance specifications of the proposed NL-PID controller when using unit step input with step disturbance of 0.2 and −0.2, and the model parameters increased by 25% from its nominal value are the rise time is 2.608, settling time is 2.608, overshoot is 0.073%, the maximum control signal is 6.230, number of slope sign change in the control signal is 231, and ITAE is 17.6064. The comparative results show the NL-PID controller's superior performance for tracking the reference signal with the lowest peak for the control signal, rejection of disturbances, ability to overcome model uncertainties, and lowest ITAE value.

Keywords: electric vehicle, nonlinear PID controller, Aquila Optimization algorithm, modelling and simulation, speed control

1 Introduction

The significance of electric vehicles (EVs) has increased over the past few decades due to global ecological concerns and energy conservation [1]. It is among the most ecologically friendly forms of transportation because it only uses renewable resources [2]. The automotive industry has focused more on research and development regarding EVs due to the growing need for technological advancements, sustainable energy use, and strict environmental safety regulations [3]. An efficient motor and intelligent control system are

* **Corresponding author: Bashra Kadhim Oleiwi**, Department of Control and System Engineering, University of Technology-Iraq, Baghdad, P.O. Box 19006, Iraq, e-mail: bushra.k.oleiwi@uotechnology.edu.iq
Mohamed Jasim Mohamed: Department of Control and System Engineering, University of Technology-Iraq, Baghdad, P.O. Box 19006, Iraq, e-mail: 60098@uotechnology.edu.iq

considered as essential elements for the quick advancements and progress of EV technology [4]. The overall effectiveness of an EV is significantly influenced by the reliability and longevity of its operating system. The DC motor is the most commonly employed in EVs due to its many advantages, which include low cost, high reliability, and easy maintenance [5]. EVs represent the future trend for their affordability and sustainability and are now considered simpler and more efficient as a result of the advances and developments made during the twentieth century [6]. Numerous research studies have concentrated on the modelling and control of EVs. EV modelling and control have been concentrated by several research studies. Different types of controllers have been utilized in EV speed control including PID controllers, fuzzy logic controllers, neural networks, etc. George and Kamath [7] designed a fractional order PID (FOPID) controller and compared the performance of the system between FOPID and integer-order PID controllers. Ann George et al. [8] provided the FOPID controller based on the Astrom–Hagglund optimization algorithm. Using Chien–Hrones–Reswick, Cohen-Coon, Ziegler–Nichols, and Astrom–Hagglund, the suggested controller gains are adjusted. George et al. [9] suggested FOPID controller with ant colony optimization and adaptive neuro-fuzzy inference system. Anshory [10] combined PID controller and bat optimization algorithm for controlling the speed of brushless direct current motor and analysing system response including overshoot and steady state value. Dantas et al. [1] applied a PID controller based on multi-parametric programming methods for regulating EV speed. The findings show that the proposed control structure can be applied to produce control actions. Bhat et al. [11] presented algorithms based on Cohen-Coon, Wang–Juang–Chan, Chine–Hrones–Reswickand PID controller for EV speed regulation. Performance indicators and comparison analysis were performed. Kaur et al. [12] introduced a PID controller with genetic algorithm to control EV speed. Ziegler–Nichols method and mean square error are compared in order to evaluate the effectiveness of the proposed method. Bisht and Yadav [13] introduced the speed control of a hybrid electric vehicle (HEV). The controller parameters are adjusted using the grey wolf and particle swarm optimization techniques. The observed results demonstrate how well the suggested strategy works to improve traffic flow and lower the HEV line's fuel consumption. Kaur et al. [14] tuned and optimized the PID controller's parameters using fuzzy logic, neural networks, and genetic algorithms to provide smooth speed tracking performance in nonlinear HEVs. Bhausaheb [15] suggested a hybrid ANN controller that combined conventional PID with ANN for SRM motor speed control in HEVs. Yadav et al. [16] designed fuzzy logic PD, fuzzy logic PI, and adaptive controllers like self-organizing controllers to control the speed of HEV. These controllers were combined with pole placement technique, observer-based controllers, linear quadratic regulator controllers, and PID controllers. Junkai et al. [17] introduced a model predictive controller to optimize the reference speed, the target speed sequence and acceleration sequence for a lower layer. The designed control strategy demonstrated robustness in different types of simulation environments. Abdulameer and Mohamed [18], Mohamed et al. [19] designed six structures of fractional order fuzzy PID controllers and neural FOPID controllers for 2-Link rigid robot manipulator. While a delivery system-based hybrid algorithm planning the optimal 3D quadcopter trajectory is introduced in the study by Kareem et al. [20]. A PID controller to regulate the EV's speed using cuckoo search optimization is applied in the study by Upadhyaya and Mahanta [21]. Mhmood et al. [22] proposed an advanced control system based on model reference control and the lead compensation for controlling the speed of the EV and improving the properties of the time response properties. dos Santos and Marques [23] presented a semi-empirical Beddoes–Leishman dynamic stall model with gust loads. The typical section equations of motion are combined with this enhanced dynamic stall model to provide a comprehensive aeroelastic framework for gust-induced stall flutter analyses. Jassim et al. [24] presented a new 4D hyper-chaotic hidden attractor system. The synchronous properties of the system are among the dynamic properties studied. Then, a synchronization scheme was designed for the proposed system and unknown system parameters were assumed. For two identical systems, a synchronization control system is implemented.

In general, the structures of the proposed controllers are designed to satisfy a certain objective function. The proposed objective function is used to minimize the ITAE and the square of the control signal as well as to satisfy the constraint on the overshoot of the response. The choice of this objective function forces the optimization algorithm to search for a solution with the fastest response and with minimum spend energy as well as near zero response overshoot for required speed. On the other side, the proposed controllers may result in control signals with high oscillations or high chattering especially when sign function is included in the controller structure as in a nonlinear NL-PID controller. A chattering signal cannot be applied practically.

Therefore, we suggest a new proposed method to make the optimization algorithm ignore or stay away from these candidate solutions. The objective function or fitness function is modified. In addition, in order to increase the training and robustness of the proposed controllers, the fitness value will consider the result of two executions simultaneously. In the first execution, we use the unit step input and disturbance input is zero while for the second execution we use unit step input and add output disturbance. By using this tuning technique, the suggested controllers will be able to reject the disturbance more quickly and effectively.

The main contributions of this work are:

1. Designing the linear and nonlinear PID controllers with the filter to control EV speed. All the proposed PID controllers are used in cascade with EV model; conventional PID controller with the filter (Con-PID), arc tan PID controller with the filter (ArcTan-PID) and nonlinear PID controller with the filter (NL-PID).
2. Applying Aquila Optimization algorithm (AOA) to determine the best values of the proposed controller gains that give the best desired performance.
3. Proposing a new tuning procedure objective function to generate a controller with the least amount of chattering in the control signal.
4. Implementing analysis of the results obtained using various control strategies using three proposed control structures for output response and control signal, and robustness towards external disturbances and model uncertainties.

The remaining sections of this article are organized as follows: EV model is described in Section 2. In Section 3, the proposed controllers are illustrated. AOA is displayed in Section 4. The simulation results and performance of the controllers are discussed in Section 5. Section 6 gives tests of robustness for all proposed controllers. Finally, the main conclusion of the research work are given in Section 7.

2 EV model description

EV avoids noise pollution due to its near-silent operation and has three primary components, namely, rechargeable battery, a controller, and an electric motor [25], as seen in Figure 1. It is powered utilizing rechargeable batteries which are essential for the use of EVs as energy storage devices [26]. The controller is to regulate the electric motor and the electric motor's input voltage is converted to the motor's rotational speed by the EV system [27]. In addition to producing high torque at low speeds, electric motors are efficient across a wider speed range [28].

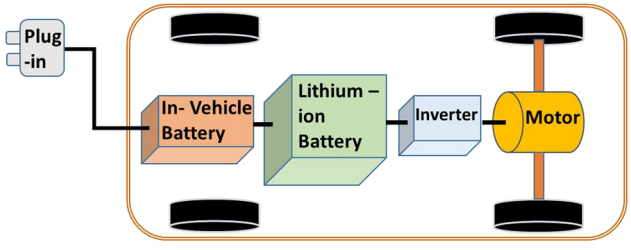

Figure 1: Block diagram of EV model.

In this work, the DC motor drives the traction system, and a suggested controller will regulate the EV's speed. Equation (1) illustrates the original model of the EV, which took into consideration the motor parameters and the road conditions, and has been defined as second order transfer function [10].

$$G(s) = \frac{k}{T^2 s^2 + 2\varepsilon T s + 1}. \tag{1}$$

The mathematical model for EV used in this study has been determined to be the stable system model in equations (2) and (3) from the study by Wicaksono and Prihatmanto [29]. The equations are as follows:

$$G(s) = \frac{0.913242}{1.39s^2 + 1.215s + 0.913242}, \tag{2}$$

or

$$G(s)\frac{0.657}{s^2 + 0.8741s + 0.657}. \tag{3}$$

To find the best control design for the EV, a comparative analysis of several control structures will need to be conducted. For the second-order transfer function of the EV, the following control structures have been proposed and used.

3 The proposed PID controllers

In this section, the proposed linear and nonlinear PID controllers are introduced. To improve the efficiency of a process control system, cascade PID control is a sophisticated form of PID control that can be implemented. Cascade control is primarily employed to quickly reject disturbances before they spread to other plant sections. All the proposed PID controllers are used in cascade with the system plant as shown in Figure 2. It depicts the SISO closed loop system's general block diagram with external disturbance, where u is the manipulated variable, d is the disturbance, e is the difference between the set-point and process output (r–y), and r is the set-point.

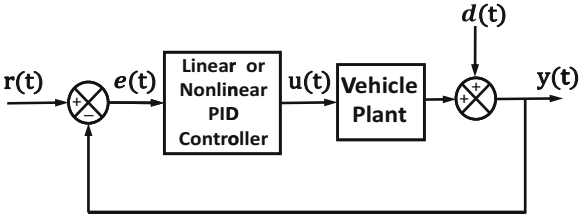

Figure 2: The block diagram of closed loop control system for linear or nonlinear PID controller applied to vehicle plant.

3.1 Con-PID

Figure 3 displays the block diagram of the traditional PID controller-based filter.

The control law of the traditional PID controller is given in equation (4).

$$u(t) = K_p e(t) + K_i \int e(t)\mathrm{d}t + K_d \frac{N}{D + N} \frac{\mathrm{d}e(t)}{\mathrm{d}t}. \tag{4}$$

3.2 ArcTan-PID controller

The ArcTan-PID control rule is defined by replacing the integral of the Arc Tan function with the error function integral in the conventional PID control rule, as shown in equation (5). The ArcTan-PID control rule is better than the conventional PID control rule in attenuating the non-constant disturbance.

$$u(t) = K_p e(t) + K_i \int \tan^{-1}(\gamma e(t))\mathrm{d}t + K_d \frac{N}{D + N} \frac{\mathrm{d}e(t)}{\mathrm{d}t}, \tag{5}$$

where γ is the design parameter.

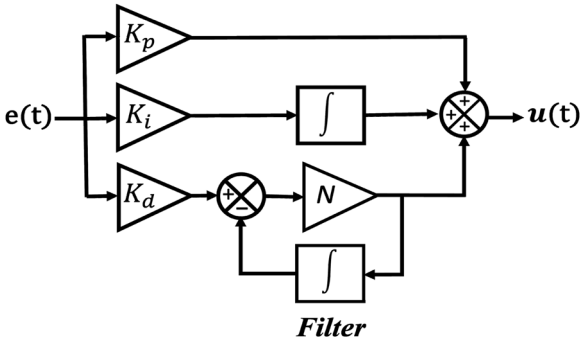

Figure 3: The traditional PID controller's block diagram.

3.3 NL-PID

By substituting a nonlinear function *f*(.) for each term in the linear PID controller. The goal of the NL-PID controller is to provide a more satisfying response to the nonlinear system. Equations (6)–(8) illustrate a nonlinear combination of the error signal's sign and exponential functions, as well as its derivative and integral.

$$u(t) = f_1(e(t)) + f_2(\dot{e}(t)) + f_3\left(\int e(t)\,\mathrm{d}t\right), \tag{6}$$

$$f_n(\beta) = k_n(\beta)|\beta|^{\alpha_n}\mathrm{sign}(\beta), \tag{7}$$

$$k_n(\beta) = k_{n1} + \frac{k_{n2}}{1 + \exp(\mu_n\beta^2)} \quad \text{for} \quad n = 1, 2, 3, \tag{8}$$

where β could be $e(t)$, $\dot{e}(t)$, or $\int e(t)\,\mathrm{d}t$, $\alpha_i \in R^+$, the function $k_n(\beta)$ is a positive function with coefficients k_{n1}, k_{n2}, and $\mu_{n1} \in R^+$. The NL-PID controller's sensitivity for small errors is increased by using the nonlinear gain term $k_n(\beta)$. The value of the nonlinear gain term $k_n(\beta)$ approaches the upper bound $k_{n1} + k_{n2}/2$ for small errors close to zero. A bounded nonlinear gain term $k_n(\beta)$ is found in the sector $[k_{n1}, k_{n1} + \frac{k_{n2}}{2}]$. While for large errors, the nonlinear gain term $k_n(\beta)$ approaches the lower bound k_{n1}.

The NL-PID controller equations are displayed in equations (9)–(16).

The error term is

$$e(t) = \mathrm{input}(t) - \mathrm{output}(t). \tag{9}$$

The derivative term is

$$\dot{e}(t) = \frac{N}{D + N}\frac{\mathrm{d}e(t)}{\mathrm{d}t}. \tag{10}$$

The proportional gain is

$$k_P(e(t)) = k_{p1} + \frac{k_{p2}}{1 + \exp(\mu_p e(t)^2)}. \tag{11}$$

The derivative gain is

$$k_d(\dot{e}(t)) = k_{d1} + \frac{k_{d2}}{1 + \exp(\mu_d \dot{e}(t)^2)}. \tag{12}$$

The integral gain is

$$k_i\left(\int e(t)\,\mathrm{d}t\right) = k_{i1} + \frac{k_{i2}}{1 + \exp(\mu_i\,(\int e(t)\,\mathrm{d}t)^2)}, \tag{13}$$

$$f_1(e) = k_p(e(t)) \times |e(t)|^{\alpha_p} \times \mathrm{sign}(e(t)), \tag{14}$$

$$f_2(\dot{e}) = k_d(\dot{e}(t)) \times |\dot{e}(t)|^{\alpha_d} \times \text{sign}(\dot{e}(t)), \tag{15}$$

$$f_3\left(\int e\,(t)\,\mathrm{d}t\right) = k_i\left(\int e(t)\,\mathrm{d}t\right) \times \left|\int e(t)\mathrm{d}t\right|^{\alpha_i} \times \text{sign}\left(\int e(t)\,\mathrm{d}t\right). \tag{16}$$

4 AOA

Aquilas are among some of the smartest and most skilled hunters, after humans [30]. Similar to how population-based algorithms work, the AOA begins with a population of candidate solutions (Pcs). With an upper (UB) and a lower (LB) limit, the method begins stochastically [31]. As shown by the equations (17)–(19), the best solution, sometimes referred to as the optimal solution, will be roughly identified after each iteration [31].

$$X = \begin{bmatrix} X_{1,1} & \cdots\cdots & X_{1,n} \\ X_{2,1} & \cdots\cdots & X_{2,n} \\ \vdots & \vdots\ \vdots & \vdots \\ X_{m,1} & X_{m,n}\ldots & X_{m,n} \end{bmatrix}, \tag{17}$$

$$X_{ij} = \text{rand} \times (\text{UB}_j - \text{LB}_j) + \text{LB}_j,\ i = 1, 2 \ldots. m,\ j = 1, 2 \ldots ..n, \tag{18}$$

where n is the problem's dimension size and m is the total population of potential solutions. The jth lower bound is LB_j if j is a random number. The jth upper bound for the given problem is UB_j. The following four steps describe AOA's simulation of an aquila's hunting behaviour:

First step: More exploration (X_1), to determine the limits of the search area and the location of the prey, the aquila explores the sky. Equations (19) and (20) illustrate how aquila locates areas of prey and chooses the optimal locations for hunting.

$$X_1(t+1) = X_{\text{best}}(t)\left(1 - \frac{t}{T}\right) + (X_M(t) - X_{\text{best}}(t) \times \text{rand}), \tag{19}$$

$$X_M(t) = \frac{1}{N}\sum_{i=1}^{N} X_i(t),\ N = 1, 2 \ldots \ldots \text{dim}, \tag{20}$$

where $X_1\,(t+1)$ represents the solution for the next iteration. Using the first search method, X_1 is produced. $X(t)$ represents the estimated point of the prey and is the best solution found up to t iteration. The supervisor's parameter for increased exploration through iteration count is $1 - tT$. The current solutions linked at the tth iteration have points mean value of t. A random value is rand. The problem's dimension size is dim. The number of people is N.

Second step: Restricted investigation X_2, the prey has been located at a considerable height. Aquila will move in this manner, circling around in the clouds, adjusting its position and preparing to attack its target. The aquila has chosen the prey area at this point. Mathematically, the second step is expressed in Equations (21–28).

$$X_2(t+1) = X_{\text{best}}(t) \times \text{Levy}(D) + X_R(t) + (y - x) \times \text{rand}, \tag{21}$$

$$\text{Levy}(D) = s \times \frac{u \times \sigma}{v^{\frac{1}{\beta}}}, \tag{22}$$

$$\sigma = \left(\frac{r(1+\beta) \times \sin\left(\frac{\pi\beta}{2}\right)}{r\left(\frac{1+\beta}{2}\right) \times \beta \times 2^{\left(\frac{\beta-1}{2}\right)}}\right), \tag{23}$$

$$y = r \times \cos(\theta), \tag{24}$$

$$x = r \times \sin(\theta), \tag{25}$$

$$r = r_1 + U + D_1, \tag{26}$$

$$\theta = -\omega \times D_1 + \theta_1, \tag{27}$$

$$\theta_1 = \frac{3 \times \pi}{2}, \tag{28}$$

where the iteration completion generated by the method's second step is represented by $X_2(t + 1)$. Levy flights have a distribution function called Levy (D). (D) is the dimension space. The value of X_R (t) is a random solution that ranges from 1 to N. The range of s, a fixed constant, is up to 0.01. Random values between 0 and 1 correspond to u and v. σ is a constant with a range of up to 1.5. In the search, the spiral shape is described by the terms x and y. A value between 1 and 20 is chosen for r_1, which is used to fix the first search cycle. The variable is equal to U times 0.00565. $D1$ is an integer with a range of 1 to the maximum value dim of the search space variable. The variable ω has a value of 0.005 multiplied by a fixed small number.

Third step: Enhanced exploitation X_3, Aquila is in an exploitative position as it approaches the target and launches a pre-emptive strike. Equation (29) is a mathematical representation of this behaviour.

$$X_3(t + 1) = (X_{\text{best}}(t) - X_R(t)) \times \alpha - \text{rand} + (\text{UB} - \text{LB}) \times \text{rand} + \text{LB} \times \delta, \tag{29}$$

where α and δ are the parameters for exploitation adjustment and have small values $(0, 1)$. For a given problem, UB and LB denote the upper and lower limit.

Fourth step: Restricted exploitation X_4, Aquilla approaches the prey more closely in fourth step. At the final location, Aquilla attacks the prey. Aquilla's behavioural modelling in fourth step can be mathematically modelled as shown in Equations (30–33).

$$X_4(t + 1) = Q_{\text{f}} \times X_{\text{best}}(t) - (G_1 \times X(t) \times \text{rand}) - G_2 \times \text{Levy}(D) + \text{rand} \times G_1, \tag{30}$$

$$Q_{\text{f}} = t^{\frac{2\times\times\text{rand}-1}{(t-r)^2}}, \tag{31}$$

$$G_1 = 2 \times \text{rand} - 1, \tag{32}$$

$$G_2 = 2 \times \left(1 - \frac{t}{T}\right), \tag{33}$$

where $X_4(t + 1)$ is the solution of the iteration produced by the fourth search method X_4. Q_{f} is the quality function that is employed to balance the search approach. Every movement type used by aquilas to track their prey is G_1. A value that decreases from 2 to 0 is called G_2. The aquila presents its flight inclination, which it uses to stick prey from the first to the last spot. The solution at the t-th iteration is t. The rand has a range of 0–1. The current iteration is t and maximum iterations is T. The flight levy's allocation function is D.

The suggested controllers' parameters in adaptive control for EV plant are optimized using the AOA, particularly at points like overshoot, rise-time, and settling-time [32]. The flowchart for AOA is displayed in Figure 4 [33]. An example of how the AOA determines the parameters of suggested controllers on an EV plant is shown in Figure 5.

5 Simulation and objectives of design

This section discusses the performance specifications of three proposed controllers (Con-PID, ArcTan-PID, and NL-PID controllers) for controlling EV speed. MATLAB is utilized for the simulation, controller design, and system modelling. The simulation results of the Con-PID, ArcTan-PID, and NL-PID controllers are compared among them as presented in the Figures 6–10, where y is the system's process output and r is the set-point. In general, the structure of the proposed controllers is designed to satisfy a certain objective function. The AOA setting for this study is 1,000 iterations as maximum number and population size is 150. The proposed controllers are tuned so as to minimize the Integral Time Absolute Error (ITAE) and integral square control signal as well as subject to constraint that the overshoot must be less than 2%. The overshoot constraint is

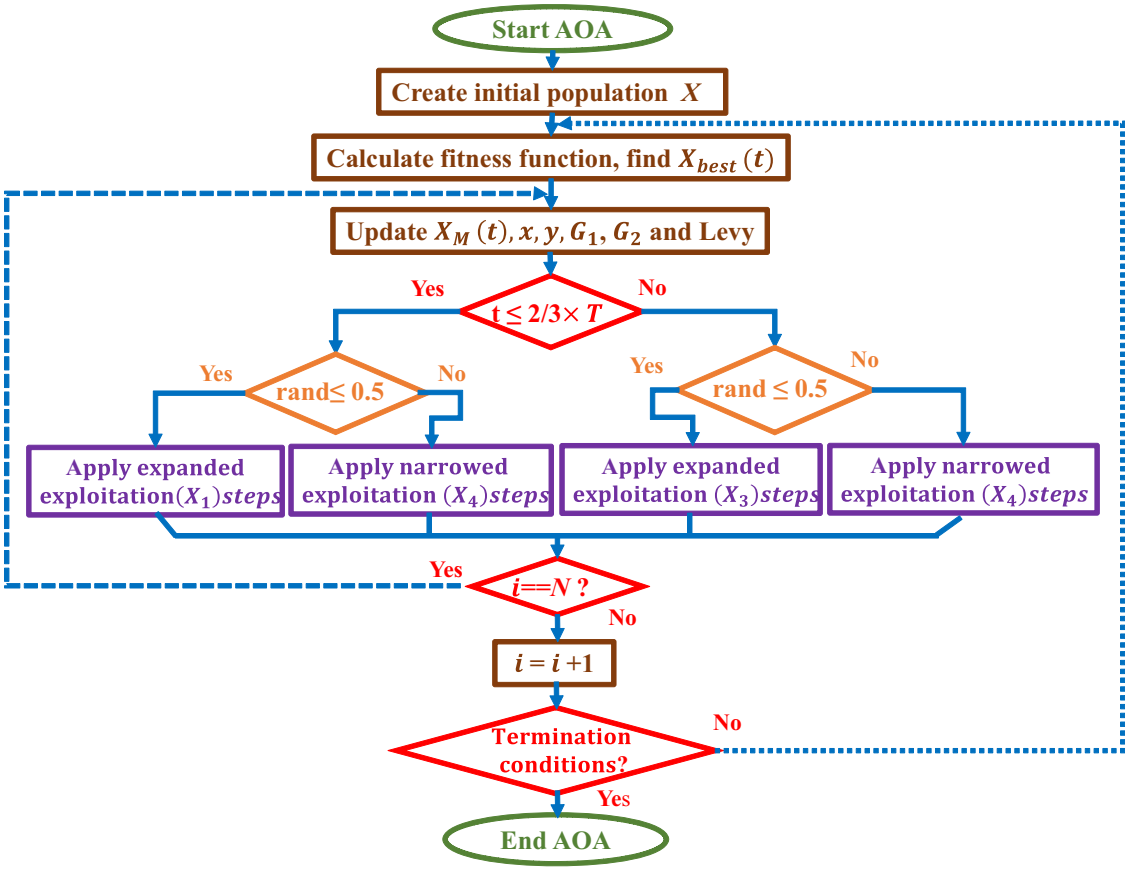

Figure 4: AOA flowchart.

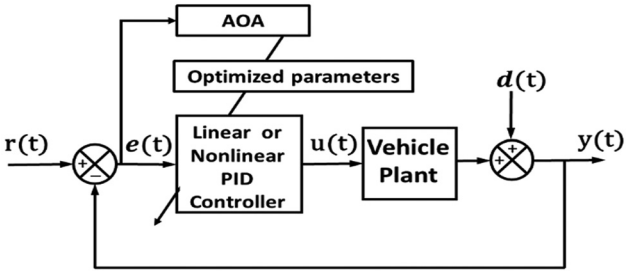

Figure 5: Block diagram of the proposed methodology.

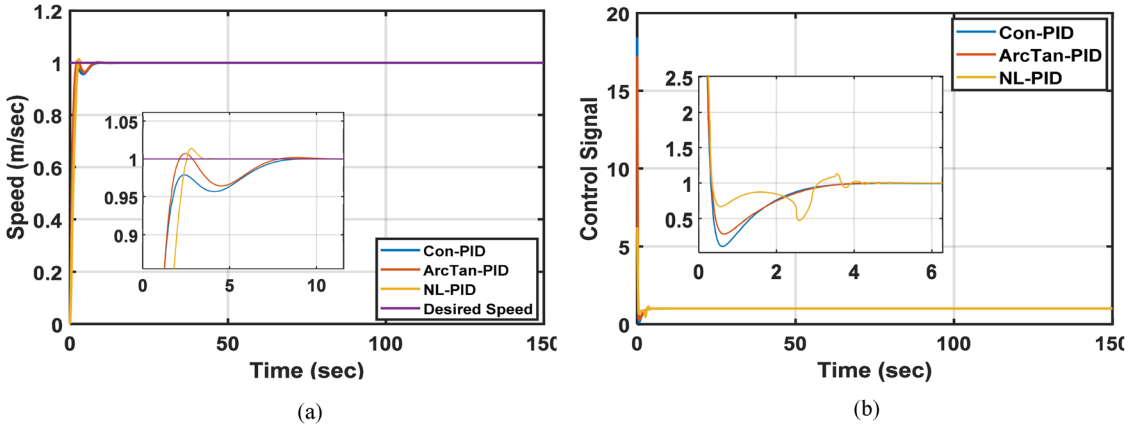

Figure 6: The performance of the proposed controllers using a unit step input with the disturbance zero. (a) The output responses and (b) the control signals.

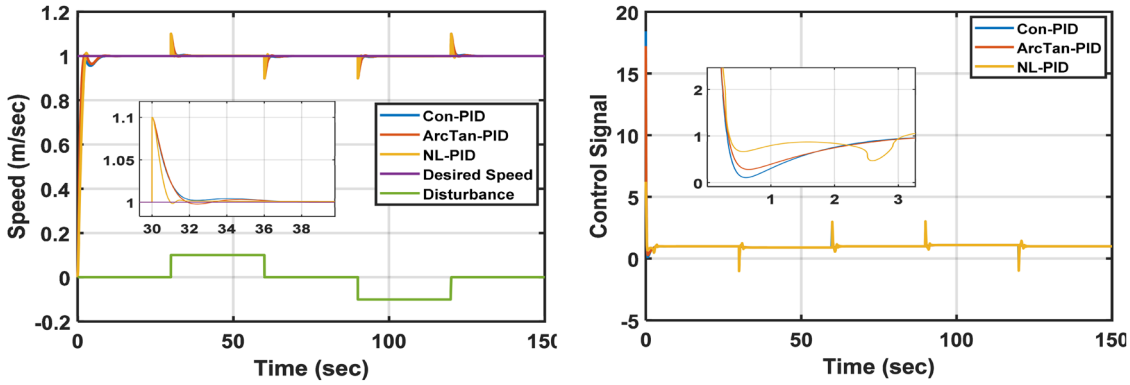

(a) (b)

Figure 7: The performance of the proposed controllers when using a unit step input with disturbance 0.1 and −0.1. (a) The output responses and (b) the control signals.

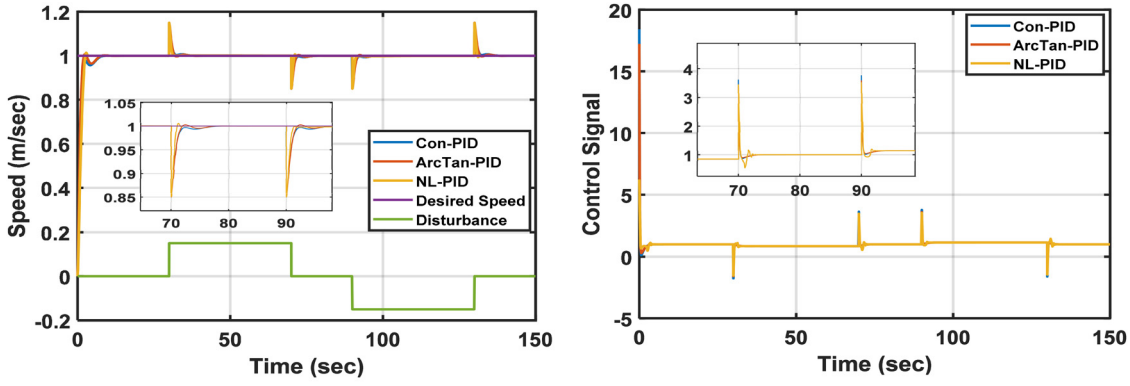

(a) (b)

Figure 8: The performance of the proposed controllers when using a unit step input with disturbance 0.15. (a) The output responses and (b) the control signals.

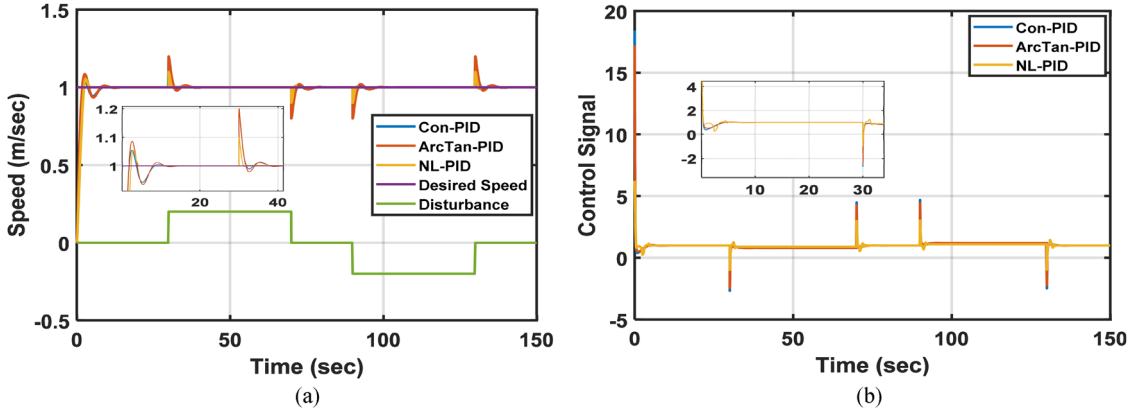

(a) (b)

Figure 9: The performance specification of the proposed controllers when using a unit step input with disturbance of 0.2 and −0.2 and the model parameters decreased by 25% from its nominal value. (a) The output responses and (b) the control signals.

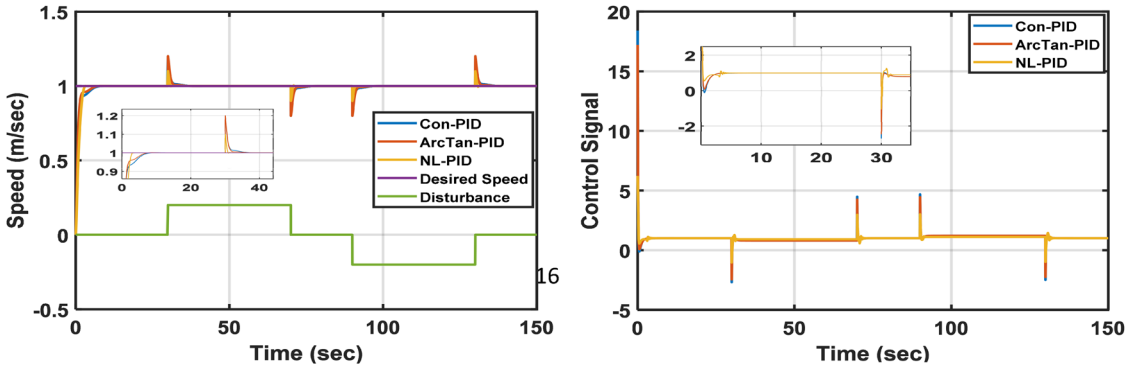

(a) (b)

Figure 10: The performance specification of the proposed controllers when using a unit step input with disturbance of 0.2 and −0.2 and the model parameters increased by 25% from its nominal value. (a) The output responses and (b) the control signals.

considered because the overshoot is a property and is not desired in output speed. The proposed objective function is shown in equation (34).

$$\min J = \int_0^{t_{ob}} (r_1 \times t \times |e(t)| + r_2 \times u^2(t))\mathrm{d}t, \quad \text{subject to constraint} \quad \text{overshoot} \quad 2\% \tag{34}$$

where $r_1 = 0.9$ and $r_2 = 0.1$ are constant weight parameters.

The technique of constant punishment is used in the evaluation of any solution, where a solution has more than 2% response overshoot will get a constant punishment as presented in equation (35).

$$\text{Punishment} = \begin{cases} 0 & \text{if overshoot } <2\% \\ 1{,}000 & \text{if overshoot } >2\% \end{cases}. \tag{35}$$

This objective function with the constraint makes the optimization algorithm searches about solution have the fastest response and minimum spend energy as well as zero overshoot in required speed. However, the proposed controllers may result in solutions with high oscillating or chattering control signals, especially when the sign function is included in the control structure as in a nonlinear NL-PID controller. In fact, a chattering signal cannot be applied practically. Therefore, we suggest new proposed method to make the optimization algorithm ignore or stay away from theses candidate solutions. The objective function or fitness function is modified as defined in equation (36).

$$\min \text{fit} = J + \rho \times \text{Fu} + \text{Punishment}, \tag{36}$$

where the minimum fit is the best, Fu is the number of times the control signal's slope changes sign, and ρ is a tiny positive number that was selected to be 10^{-2}.

In addition, in order to increase the training and robustness of the proposed controllers the fitness value will consider the result of two executions simultaneously, in the first execution, we use the unit step input and disturbance input is zero while for the second execution we use unit step input and add output disturbance as described in equation (37).

$$d(t) = \begin{cases} 0.1 & 60\langle \text{time} \rangle 30 \\ -0.1 & 120\langle \text{time} \rangle 90 \\ 0 & \text{elsewhere} \end{cases}. \tag{37}$$

This tuning method will increase the proposed controller's capability to reject disturbance quickly and efficiently.

The search spaces of all controllers' parameters are shown in Table 1, while the optimal controller's parameters found by AOA for all controllers are shown in Table 2. The performance specifications of all proposed PID controllers are illustrated in Table 3 when using unit step input with the disturbance zero. These performance specifications are the rising time, settling time, maximum control signal, number of slope sign change, and the ITAE value. Figure 6 depicts the performance of all suggested controllers in terms of output responses and control signals when unit step input is used with the disturbance zero.

From these results, it can be seen that NL-PID controller gives smoother output response without undershoot, faster convergence to the reference signal, and a control signal with least oscillation. In addition, its

Table 1: Search spaces of all proposed controllers' parameters

Controller type	K_p	K_i	K_d	N	γ
Con-PID	0–2	0–2	0–2	10–100	—
ArcTan-PID	0–2	0–2	0–2	10–100	1 to 50
NL-PID	K_{p1}	K_{i1}	K_{d1}	10–100	—
	0–1	0–1	0–1		
	K_{p2}	K_{i2}	K_{d2}		
	0–1	0–1	0–1		
	μ_p	μ_i	μ_d		
	0–2	0–2	0–2		
	α_p	α_i	α_p		
	0–1	0–1	0–1		

Table 2: Optimal parameters of all proposed controllers

Controller type	K_p	K_i	K_d	N	γ
Con-PID	2.0	1.178065	1.649769	10.0	—
ArcTan-PID	2.0	2.0	1.528760	10.0	0.6691
NL-PID	K_{p1}	K_{i1}	K_{d1}	10.0	—
	1.0	1.0	1.0		
	K_{p2}	K_{i2}	K_{d2}		
	1.0	0.01407	1.0		
	μ_p	μ_i	μ_d		
	0.14374	0.41087	0.015		
	α_p	α_i	α_p		
	0.44533	1.0	0.60583		

Table 3: Performance specification of the suggested controllers when using a unit step input with the disturbance zero

Controller type	Rise time	Settling time	Maximum control signal	Number of slope sign change in control signal	ITAE
Con-PID	6.059	6.059	18.416	499	1.039479
ArcTan-PID	1.837	5.932	17.212	562	0.861674
NL-PID	2.362	2.362	6.2306	33	1.151145

response has minimum settling time equal to 2.362 s and minimum peak of control signal 6.2306 as compared with the other controllers. In spite the NL-PID controller gives an ITAE equal to 1.151145 which is more than

ArcTan-PID's ITAE = 0.861674 and Con-PID's ITAEs = 1.039479, but the NL-PID controller's performance is better than them.

Now, to verify the proposed controller's performance with a unit step input reference and the disturbance input is like in equation (37). The performance specifications of the proposed controllers like rise time, settling time, and maximum control signal are the same as the case when disturbance is zero while the value of the number of slope sign change in control signal and ITAE value are altered as shown in Table 4. In Figure 7 the output responses and control signals of all proposed controllers are shown.

From the obtained results, the suggested NL-PID controller still gives least ITAE value, reasonable oscilla-

Table 4: Performance specifications of the proposed controllers using unit step input reference with disturbance as shown in equation (37)

Controller type	Number of slope sign change in control signal	ITAE
Con-PID	103	26.94318
ArcTan-PID	58	24.96070
NL-PID	171	16.96852

tion of control signal, and the response rabidly coverage to the desired set point value when disturbance is added to the output speed. Therefore, the suggested NL-PID controller outperforms the other proposed controllers for disturbance rejection.

5.1 Robustness test

Now, in order to check the robustness of the proposed PID controllers against a variation in the system's parameters and a hard output disturbance without returning the proposed controller's parameters. All the proposed controllers submit the following robustness tests.

5.1.1 Disturbance addition test

A unit step is used in a reference input and a constant disturbance with value 0.15 is added to the output response in the period from 30 to 70 and with the value −0.15 in the period 90–130. Table 5 displays the number of slope sign changes in the control signal as well as the ITAE value for each suggested controller. The output responses and control signals for each suggested controller are shown in Figure 8.

Based on the results, it can be noted that the number of slope sign change in control signal and the ITAE's

Table 5: Performance specification of the proposed controllers, when using a unit step input with disturbance of 0.15 and −0.15

Controller type	Number of slope sign change in control signal	ITAE
Con-PID	3,253	42.44383
ArcTan-PID	508	39.38920
NL-PID	117	31.85110

value for the NL-PID controller are less than another proposed controller. In addition, the output converges to the desired output value rapidly due to a change in the input signal or the effect of output disturbance. The

worst controller is Con-PID since it has the largest ITAE's value and its response has a largest settling time as well as a high chattering in its control signal.

5.1.2 Disturbance addition and decreasing system's parameters test

In this test, the parameters of the system decrease by 25% from their nominal values where the transfer function of the system assume to become as depicted in equation (38). In addition, a constant output disturbance of a value 0.2 is added in a period 30–70 and disturbance of a value −0.2 in a period 90–130 while the reference input is unit step.

$$G(s) = \frac{0.4928}{s^2 + 0.6556s + 0.4928}. \tag{38}$$

The performance specifications of each proposed controller are shown in Table 6. The output responses and control signals of each proposed controller are shown in Figure 9.

Table 6: Performance specification of the proposed controllers when using a unit step input with disturbance of 0.2 and −0.2 and the model parameters decreased by 25% from its nominal value

Controller type	Rise time	Settling time	Overshoot %	Maximum control signal	Number of slope sign change in control signal	ITAE
Con-PID	1.778	7.186	5.446	18.416	54	66.39593
ArcTan-PID	1.723	7.146	8.612	17.212	52	74.11338
NL-PID	2.271	3.741	5.506	6.2306	157	21.85286

From the result shown in Table 6, we notice that the NL-PID has the smallest settling time, best overshoot, least peak in control signal, and least ITAE. The number of slope sign change in control signal and the rise time value for NL-PID controller are reasonable. In addition, Figure 9 shows the effect of disturbance on the output response and the control signal is smallest for NL-PID controller compared with the other proposed controllers.

5.1.3 Disturbance addition and increasing system's parameters test

In this test, the parameters of the system increase by 25% from their nominal values where the transfer function of the system is assumed to become as illustrated in equation (39). Also, a constant output disturbance of a value 0.2 is added in a period 30–70 and disturbance of a value −0.2 in a period 90–130 while the reference input is unit step.

$$G(s) = \frac{0.8213}{s^2 + 1.0926s + 0.8213}. \tag{39}$$

In Table 7, the performance specifications for all the proposed controllers are illustrated. The output responses and control signals for all the proposed controllers are shown in Figure 10. The comparative results show the NL-PID controller's superior performance for tracking the reference signal with minimum peak for the control signal, rejection of disturbances, ability to overcome model uncertainties, and minimum ITAE value. The performance specifications of the proposed NL-PID controller when using a unit step input with disturbance of 0.2 and −0.2 and the model parameters increased by 25% from its nominal value, i.e., rise time to 2.608, settling time to 2.608, overshoot to 0.073%, maximum control signal to 6.230, number of slope sign change in control signal to 231, and ITAE to 17.6064.

Table 7: Performance specification of each proposed controller when using a unit step input with disturbance of 0.2 and −0.2 and the model parameters increased by 25% from its nominal value

Controller type	Rise time	Settling time	Overshoot %	Maximum control signal	Number of slope sign change in control signal	ITAE
Con-PID	5.367	5.367	0.032	18.416	6297	56.32753
ArcTan-PID	4.847	4.847	0.067	17.212	5136	49.4574
NL-PID	2.608	2.608	0.073	6.230	231	17.6064

The results in Table 6 show that the NL-PID has a smallest rise time, a smallest settling time, zero overshoot, least peak in control signal, small number of slope sign change in control signal, and least ITAE. In addition, Figure 10 shows the effect of disturbance on the output response and control signal is the smallest for NL-PID controller compared with other proposed controllers.

Now, returning to all previous tests on the proposed controllers, we conclude that the NL-PID controller is the best in all these tests and superior to other proposed controller.

6 Conclusion

In order to control the speed of the EV, this work focuses on designing three different control structures, including linear and nonlinear PID controllers. The proposed controllers are Con-PID, ArcTan-PID, and NL-PID controllers, which are used in cascade with second-order transfer function model. The parameters tuning of the proposed controllers is achieved by AOA according to the proposed performance index and constraint. Numerical simulation, system modelling and controller design are done using MATLAB. After the proposed controllers were design completely, they were subjected to three robustness tests. A comparative study has been carried out to evaluate the performance of the proposed controllers for determining the best control algorithm. Simulation results proved that the proposed NL-PID controller outperforms the other proposed controllers for output response, control signal, and robustness. The performance specifications of the proposed NL-PID controller using unit step input with disturbance of 0.2 and −0.2 and the model parameters increased by 25% from its nominal value, i.e., rise time to 2.608, settling time to 2.608, overshoot to 0.073 %, maximum control signal to 6.230, number of slope sign change in control signal to 231, and ITAE to 17.6064. The NL-PID controller is the best one for tracking reference signal, disturbances rejection, and to overcome the model uncertainties with minimum value of performance index ITAE. Finally, other approaches could be used in future work to improve system efficiency, such as using a cascaded controller architecture, intelligent technology combined with a conventional controller, or a more modern optimization algorithm that can provide better tunable gain values that can be used to improve system performance. Also, as a suggestion for future work, it is possible to implement the proposed design practically on a real robot with the required tools, e.g., sensors and microcontrollers. The proposed technique can be extended and applied to other electro-mechanical under-actuated systems.

Funding information: Researchers received no external funding.

Author contributions: Conceptualization, Mohamed Jasim Mohamed and Bashra Kadhim Oleiwi; Methodology, Mohamed Jasim Mohamed and Bashra Kadhim Oleiwi; Software, Mohamed Jasim Mohamed; Validation, Bashra Kadhim Oleiwi; Formal analysis, Mohamed Jasim Mohamed and Bashra Kadhim Oleiwi; Investigation, Bashra Kadhim Oleiwi; Resources, Mohamed Jasim Mohamed and Bashra Kadhim Oleiwi; Writing – original draft, Mohamed Jasim Mohamed and Bashra Kadhim Oleiwi; Writing – review & editing, Mohamed Jasim Mohamed and Bashra Kadhim Oleiwi; Visualization. All authors have read and agreed to the published version of the manuscript.

Conflict of interest: The authors declare that they have no conflict of interest.

Data availability statement: The original contributions presented in the study are included in the article; further inquiries can be directed to the corresponding author.

References

[1] Dantas ADODS, Dantas AFODA, Campos JTL, de Almeida Neto DL, Dórea CET. PID control for electric vehicles subject to control and speed signal constraints. J Control Sci Eng. 2018;2018:11. Article ID 6259049. doi: 10.1155/2018/6259049.

[2] Oleiwi BK, Mahfuz A, Roth H. Application of fuzzy logic for collision avoidance of mobile robots in dynamic-indoor environments. 2nd International Conference on Robotics, Electrical and Signal Processing Techniques 2021 (ICREST 2021) organized by Faculty of Engineering, American International University-Bangladesh (AIUB); 2021. doi: 10.1109/ICREST51555.2021.9331072.

[3] Khooban MH, ShaSadeghi M, Niknam T, Blaabjerg F. Analysis, control and design of speed control of electric vehicles delayed model: Multi-objective fuzzy fractional-order PIkDl controller. IET. 2017.

[4] Yong JY, Ramachandaramurthy VK, Tan KM, Mithulananthan N. A review on the state-of-the-art technologies of electric vehicle, its impacts and prospects. Renew Sustain Energy Rev. 2015;49:365–85. doi: 10.1016/j.rser.2015.04.130.

[5] Oleiwi BK. Scouting and controlling for mobile robot based raspberry PI 3. J Comput Theor Nanosci. 2019 Jan;16(1):79–83(5). doi: 10.1166/jctn.2019.7701.

[6] Bova N, Marrs Z, Goodwin J, Oliva A. Environmental and Social Issues Concerned with Hybrid Cars. 2010;1–120.

[7] George MA, Kamath DV. Design and tuning of fractional order PID (FOPID) controller for speed control of electric vehicle on concrete roads. 2020 IEEE International Conference on Power Electronics, Smart Grid and Renewable Energy (PESGRE2020), Cochin, India; 2020. p. 1–6. doi: 10.1109/PESGRE45664.2020.9070457.

[8] Ann George M, Durga Bhavani IVL, Kamath DV. EX-CCII based FOPID controller for electric vehicle speed control. 2020 IEEE International Conference on Distributed Computing, VLSI, Electrical Circuits and Robotics (DISCOVER), Udupi, India; 2020. p. 47–51. doi: 10.1109/DISCOVER50404.2020.9278055.

[9] George MA, Kamat DV, Kurian CP. Electric vehicle speed tracking control using an ANFIS-based fractional order PID controller. J King Saud Univ – Eng Sci. 2022;36(4):256–64. doi: 10.1016/j.jksues.2022.01.001.

[10] Anshory MI. Performance analysis stability of speed control of BLDC motor using PID-BAT algorithm in electric vehicle. J Electr Electron Eng UMSIDA. 2017 Apr;1(1):22–8. doi: 10.21070/jeee-u.v1i1.757. Performance analysis stability of speed control of BLDC motor using PID-BAT algorithm in electric vehicle.

[11] Bhat VS, Shettigar AG, Nikhitha, Dayanand N, Vishal Kumar KP. Analysis of PID control algorithms for transfer function model of electric vehicle. Int J Recent Technol Eng. 2019 Jun;8(1S4):1022–6.

[12] Kaur J, Saxena P, Gaur P. Genetic algorithm based speed control of hybrid electric vehicle. 2013 Sixth International Conference on Contemporary Computing (IC3), Noida, India; 2013. p. 65–9. doi: 10.1109/IC3.2013.6612163.

[13] Bisht P, Yadav J. Optimal speed control of hybrid electric vehicle using GWO based fuzzy-PID controller. 2020 International Conference on Advances in Computing, Communication & Materials (ICACCM), Dehradun, India; 2020. p. 115–20. doi: 10.1109/ICACCM50413.2020.9212985.

[14] Kaur J, Gaur P, Saxena P, Kumar V. Speed control of hybrid electric vehicle using artificial intelligence techniques. Int J Comput. 2014;2:33–9.

[15] Bhausaheb RM. Speed control of SRM for hybrid electric vehicle using artificial intelligence. 2021 12th International Conference on Computing Communication and Networking Technologies (ICCCNT), Kharagpur, India; 2021. p. 1–5. doi: 10.1109/ICCCNT51525.2021.9579857.

[16] Yadav A, Gaur P, Jha S, Gupta JRP, Mittal A. Optimal speed control of hybrid electric vehicles. J Power Electron. 2011;11:393–400. doi: 10.6113/JPE.2011.11.4.393.

[17] Junkai Y, Jinju S, Xunyi L, Kangjian Y. Speed planning and energy optimal control of hybrid electric vehicles based on internet of vehicles. IFAC-PapersOnLine. 2021;54(10):169–75. doi: 10.1016/j.ifacol.2021.10.159.

[18] Abdulameer HI, Mohamed MJ. Fractional order fuzzy PID controller design for 2-link rigid robot manipulator. Int J Intell Eng Syst. 2022;15(3):103–17. doi: 10.22266/ijies2022.0630.10.

[19] Mohamed MJ, Oleiwi BK, Abood LH, Azar AT, Hameed IA. Neural fractional order PID controllers design for 2-link rigid robot manipulator. Fractal Fract. 2023;7:693. doi: 10.3390/fractalfract7090693.

[20] Kareem AA, Oleiwi BK, Mohamed MJ. Planning the optimal 3D quadcopter trajectory using a delivery system-based hybrid algorithm. Int J Intell Eng Syst. 2023;16(2):427–39. doi: 10.22266/ijies2023.0430.34.

[21] Upadhyaya A, Mahanta C. Speed control of electric vehicle considering topographic data. 2022 IEEE Delhi Section Conference (DELCON), New Delhi, India; 2022. p. 1–7. doi: 10.1109/DELCON54057.2022.9752909.

[22] Mhmood A, Oleiwi B, Rakan A. Optimal model reference lead compensator design for electric vehicle speed control using zebra optimization technique. Jordan J Mech Ind Eng. 2023;17:533–40. doi: 10.59038/jjmie/170408.

[23] dos Santos LGP, Marques FD. Nonlinear aeroelastic analysis of airfoil section under stall flutter oscillations and gust loads. J Fluids Struct. 2021;102:103250. doi: 10.1016/j.jfluidstructs.2021.103250.

[24] Jasim BH, Hassan KH, Omran KM. A new 4-D hyperchaotic hidden attractor system: Its dynamics, coexisting attractors, synchronization and microcontroller implementation. Int J Electr Comput Eng. 2021 Jun;11(3):2068–78. doi: 10.11591/ijece.v11i3.pp2068-2078.
[25] Guozhen HU, ShanxuDuan, Tao CAI, Baoqi LIU. Modeling, control and implementation of lithium-ion-battery charger in electric vehicle application. Electr Rev. 2012;88(1):255–8.
[26] Abood LH, Oleiwi BK, Humaidi AJ, Al-Qassar AA, Al-Obaidi ASM. Design a robust controller for congestion avoidance in TCP/AQM system. Adv Eng Softw. 2023 Mar;176:103395. doi: 10.1016/j.advengsoft.2022.103395. https://www.sciencedirect.com/science/article/abs/pii/S0965997822002964.
[27] Farhan A. Salem. Modeling and control solutions for electric vehicles. Eur Sci J. 2013;9:221–40.
[28] Oleiwi BK, Al-Jarrah R, Roth H, Kazem BI. Integrated motion planning and control for multi objectives optimization and multi robots navigation. The 2nd IFAC Conference on Embedded Systems, Computer Intelligence and Telematics (CESCIT 2015), Maribor, Slovenia, 22–24 June, 2015. IFAC-PapersOnLine. Vol. 48, No. 10. Amsterdam: Elsevier Ltd; 2015. p. 99–104.
[29] Wicaksono A, Prihatmanto AS. Optimal control system design for electric vehicle. 4th International Conference on Interactive Digital Media, Indonesia; 2015.
[30] Abualigah L. Aquila optimizer: A novel meta-heuristic optimization algorithm. Comput Ind Eng. 2021;157(107250). doi: 10.1016/j.cie.2021.107250.
[31] Oleiwi BK, Roth H, Kazem BI. Multi objective optimization of path and trajectory planning for non-holonomic mobile robot using enhanced genetic algorithm. Proceedings of the 8th International Conference on Neural Networks and Artificial Intelligence (ICNNAI 2014), Brest, Belarus, 3–6 June, 2014. Published in: Communications in Computer and Information Science, Springer International Publishing, vol. 440; 2014. pp. 50–62.
[32] Aribowo W, Supari S, Suprianto B. Optimization of PID parameters for controlling DC motor based on the aquila optimizer algorithm. Int J Power Electron Drive Syst. 2022 Mar;13(1):216–22. doi: 10.11591/ijpeds.v13.i1.pp216-222.
[33] Akyol S. A new hybrid method based on Aquila optimizer and tangent search algorithm for global optimization. J Ambient Intell Hum Comput. 2023;14:8045–65. doi: 10.1007/s12652-022-04347-1.